Published in final edited form as:

Neuron. 2020 April 22; 106(2): 237–245.e8. doi:10.1016/j.neuron.2020.01.027.

Pathogenic Variants in CEP85L Cause Sporadic and Familial Posterior Predominant Lissencephaly

Meng-Han Tsai[1,2,25], **Alison M. Muir**[3,25], **Won-Jing Wang**[4], **Yi-Ning Kang**[5], **Kun-Chuan Yang**[5], **Nian-Hsin Chao**[5], **Mei-Feng Wu**[4], **Ying-Chao Chang**[6], **Brenda E. Porter**[7], **Laura A. Jansen**[8], **Guillaume Sebire**[9], **Nicolas Deconinck**[10], **Wen-Lang Fan**[11], **Shih-Chi Su**[12], **Wen-Hung Chung**[2,12,13], **Edith P. Almanza Fuerte**[3], **Michele G. Mehaffey**[3], **University of Washington Center for Mendelian Genomics**, **Ching-Ching Ng**[14], **Chung-Kin Chan**[14], **Kheng-Seang Lim**[15], **Richard J. Leventer**[16,17], **Paul J. Lockhart**[16,17], **Kate Riney**[18], **John A. Damiano**[16,19], **Michael S. Hildebrand**[16,19], **Ghayda M. Mirzaa**[3,20,21], **William B. Dobyns**[3,20,21], **Samuel F. Berkovic**[19], **Ingrid E. Scheffer**[16,17,19,22], **Jin-Wu Tsai**[5,23,24,25,26,*], **Heather C. Mefford**[3,21,25,*]

[1]Department of Neurology, Kaohsiung Chang Gung Memorial Hospital, Kaohsiung, Taiwan 833, ROC

[2]School of Medicine, College of Medicine, Chang Gung University, Taoyuan, Taiwan 33302, ROC

[3]Department of Pediatrics, University of Washington, Seattle, WA 98195, USA

[4]Institute of Biochemistry and Molecular Biology, College of Life Science, National Yang-Ming University, Taipei, Taiwan, ROC

[5]Institute of Brain Science, School of Medicine, National Yang-Ming University, Taipei, Taiwan, ROC

[6]Department of Pediatrics, Kaohsiung Chang Gung Memorial Hospital, Chang Gung University College of Medicine, Kaohsiung, Taiwan, ROC

[7]Department of Neurology, Stanford University School of Medicine, Palo Alto, CA, USA

[*]Correspondence: tsaijw@ym.edu.tw (J.-W.T.), hmefford@uw.edu (H.C.M.).

AUTHOR CONTRIBUTIONS

M.-H.T., A.M.M., J.-W.T., and H.C.M. designed the study. M.-H.T., A.M.M., E.P.A.F., M.G.M., W.-L.F., S.-C.S., W.-H.C., P.J.L., UWCMG, J.A.D., and M.S.H. supported the sequencing and variant interpretation. M.-H.T., B.E.P., L.A.J., G.S., N.D., G.M.M., R.J.L., K.R., S.F.B., I.E.S., W.B.D., Y.-C.C., and H.C.M. collected and analyzed the clinical data and/or provided patients' samples. J.-W.T, W.-J.W., Y.-N.K., K.-C.Y., N.H.C., and M.-F.W. performed the CEP85L functional analysis. M.-H.T., A.M.M., J.-W.T., and H.C.M. wrote the manuscript, with contributions from W.-J.W., S.F.B., and I.E.S. All authors contributed to and critically reviewed the manuscript.

SUPPLEMENTAL INFORMATION

Supplemental Information can be found online at https://doi.org/10.1016/j.neuron.2020.01.027.

DECLARATION OF INTERESTS

N.D. has served on scientific advisory boards for Sarepta, Biomarin, and Avexis. I.E.S. has served on scientific advisory boards for UCB, Eisai, GlaxoSmithKline, BioMarin, Nutricia, Rogcon, and Xenon Pharmaceuticals; editorial boards of the *Annals of Neurology*, *Neurology*, and *Epileptic Disorders*; may accrue future revenue on pending patent WO61/010176 (filed: 2008): Therapeutic Compound; has received speaker honoraria from GlaxoSmithKline, Athena Diagnostics, UCB, BioMarin, and Eisai; and has received funding for travel from Athena Diagnostics, UCB, Biocodex, GlaxoSmithKline, Biomarin, and Eisai. H.C.M. is a member of scientific advisory boards for Lennox Gastaut Syndrome Foundation, Dravet Syndrome Foundation, and SPARK. K.R. has served on advisory boards for UCB, Eisai, Liva Nova, and Novartis; has received research funding from UCB, Jansen-Cilag, Novartis, Zogenix, Liva Nova, Eisai, and AFT Pharmaceuticals; and received speaker honoraria from UCB and Biomarin. All other authors declare no competing interests.

[8]Department of Neurology, Washington University School of Medicine, St. Louis, MO, USA

[9]Department of Pediatrics, McGill University, Montreal, QC, Canada

[10]Department of Paediatric Neurology, Hôpital Universitaire des Enfants Reine Fabiola, HUDERF, Université Libre de Bruxelles (ULB), Brussels, Belgium

[11]Genomic Medicine Core Laboratory, Chang Gung Memorial Hospital, Linkou, Taiwan, ROC

[12]Whole-Genome Research Core Laboratory of Human Diseases, Chang Gung Memorial Hospital, Keelung, Taiwan, ROC

[13]Department of Dermatology, Drug Hypersensitivity Clinical and Research Center, Chang Gung Memorial Hospital, Linkou, Taipei and Keelung, Taiwan, ROC

[14]Genetics and Molecular Biology, Institute of Biological Sciences, Faculty of Science, University of Malaya, Kuala Lumpur, Malaysia

[15]Division of Neurology, Faculty of Medicine, University of Malaya, Kuala Lumpur 50603, Malaysia

[16]Murdoch Children's Research Institute, Royal Children's Hospital, Parkville 3052, VIC, Australia

[17]Departments of Paediatrics and Neurology, The Royal Children's Hospital, The University of Melbourne, Melbourne 3052, VIC, Australia

[18]Neurosciences Unit, Queensland Children's Hospital and School of Medicine, University of Queensland, Brisbane 4101, QLD, Australia

[19]Epilepsy Research Centre, University of Melbourne, Austin Health, Melbourne 3084, VIC, Australia

[20]Center for Integrative Brain Research, Seattle Children's Research Institute, Seattle, WA 98105, USA

[21]Brotman Baty Institute for Precision Medicine, Seattle, WA, USA

[22]The Florey Institute of Neuroscience and Mental Health, Melbourne 3052, VIC, Australia

[23]Brain Research Center, National Yang-Ming University, Taipei 112, Taiwan, ROC

[24]Department of Biological Science & Technology, National Chiao Tung University, Hsin-Chu 30010, Taiwan, ROC

[25]These authors contributed equally

[26]Lead Contact

SUMMARY

Lissencephaly (LIS), denoting a "smooth brain," is characterized by the absence of normal cerebral convolutions with abnormalities of cortical thickness. Pathogenic variants in over 20 genes are associated with LIS. The majority of posterior predominant LIS is caused by pathogenic variants in *LIS1* (also known as *PAFAH1B1*), although a significant fraction remains without a known genetic etiology. We now implicate CEP85L as an important cause of posterior predominant LIS, identifying 13 individuals with rare, heterozygous *CEP85L* variants, including 2 families with autosomal dominant inheritance. We show that CEP85L is a centrosome protein

localizing to the pericentriolar material, and knockdown of *Cep85l* causes a neuronal migration defect in mice. LIS1 also localizes to the centrosome, suggesting that this organelle is key to the mechanism of posterior predominant LIS.

In Brief

Tsai et al. implicate *CEP85L* as an important cause of posterior predominant lissencephaly, identifying 13 individuals with rare, heterozygous *CEP85L* variants, including 2 families with autosomal dominant inheritance.

INTRODUCTION

Lissencephaly (LIS), denoting a “smooth brain,” is characterized by excessive cortical thickness with reduced cerebral convolutions. Radiological patterns are classified according to a spectrum of severity (agyria, pachygyria, and subcortical band heterotopia [SBH]), topographical distribution (e.g., anterior, posterior, and diffuse), and associated abnormalities (Di Donato et al., 2017). Patients typically present with developmental delay and intractable epilepsy. Pathogenic variants in over 20 genes are associated with LIS. The majority of posterior predominant LIS is caused by variants in *LIS1* (also known as *PAFAH1B1*), although a significant fraction remains without an identified genetic etiology (Di Donato et al., 2018).

RESULTS

Exome and Targeted Sequencing Identify Rare, Heterozygous Variants in CEP85L in Individuals with Posterior Dominant LIS

We identified rare, heterozygous, *de novo* and inherited variants in *CEP85L* (GenBank: NM_001042475.3) in 13 subjects from 9 unrelated families with posterior predominant LIS, intractable seizures, and developmental delay (Figures 1 and S1; Tables 1 and S1). The initial discovery came from the identification of *de novo* or rare heterozygous variants in five unrelated subjects and one affected family member (individuals I, III, IV, VII, IX-a, and IX-b) by exome sequencing. The remainder of the patients were identified by targeted sequencing of a cohort of 31 individuals with SBH (n = 6/31) and a search of the literature (n = 1) (Deciphering Developmental Disorders, 2017).

Two unrelated individuals have different *de novo* CEP85L:p. (Met1?) variants (I and II). There are two full-length transcripts of *CEP85L* (GenBank: NM_001042475 and NM_001178035), which differ in their 5′ UTRs and first coding exons and have alternative start codons. The p.(Met1?) variants identified in these individuals affect only the NM_001042475 transcript. RNA sequencing (RNA-seq) showed that NM_001042475 is the predominant transcript in all tissues tested, including fetal brain (Figure S2A). Furthermore, we determined by western blot that the CEP85L protein was markedly decreased in lymphoblastoid cells derived from individual I, who harbored the p.(Met1?) variant, compared to control (Figure S2B). To confirm the consequence of the p.(Met1?) variant on CEP85L protein abundance, we expressed a FLAG-tagged *CEP85L* NM_001042475:c.2T > C construct in HEK293T cells and showed that the abundance of CEP85L p.(Met1?) was

dramatically decreased compared to control CEP85L (Figure S2C). The size of the remaining CEP85L:p.(Met1?) was reduced from ~100 kDa to ~80 kDa, consistent with use of a second downstream in-frame methionine, p.(Met103), as an alternative start codon.

Two sisters (IX-a and IX-b) shared an apparently *de novo* c.232+5G > A variant, suggesting parental mosaicism, especially given that the sisters are not twins. We were unable to detect the variant in either parent despite targeted deep sequencing (Myers et al., 2018), suggesting gonadal mosaicism. This variant was located near the splice donor site of the second exon of the *CEP85L* NM_001042475 transcript. RNA expression studies using blood-derived RNA from both sisters showed that exon 2 was skipped in approximately 10% of transcripts, an aberrant splicing event not seen in control leukocytes (Figure S3). Exon 2 skipping is predicted to result in an in-frame deletion of 53 amino acids (aa), namely, variant p.(Gly25_Glu77del).

We identified nearby splice-site variants c.232+1G > T and c.232+3G > T in individual VII and an affected father-daughter pair (VIII-a and VIII-b), respectively. Both variants are also predicted to cause a loss of the splice donor site from exon 2 (Desmet et al., 2009). Although we were unable to evaluate RNA, we hypothesize that these variants will result in skipping of exon 2, similar to c.232+5G > A.

Likely Pathogenic Missense Variants in CEP85L Cluster in a Highly Constrained Coding Region

Six individuals from four families had rare missense variants in *CEP85L*: p.(Ser58Cys), p.(Asp65Asn), p.(Ile68Thr), and p.(Glu69Arg). On a gene-wide level *CEP85L* is tolerant to missense variation (*Z* score = 0.4) (Lek et al., 2016), whereas the variants in these four families are contained within a 15-aa highly constrained coding region (>95th percentile) (Havrilla et al., 2019) in the second exon of the *CEP85L* NM_001042475 transcript. Two of the missense variants were identified by targeted sequencing of *CEP85L* in 27 unrelated individuals with SBH, representing a highly significant enrichment of variants in this region in cases compared to healthy individuals (2/54 alleles versus 2/31,400 alleles in Genome Aggregation Database [gnomAD]; $p < 0.00001$, two-sided chi-square test). The predicted protein products of the c.232+5G > A, c.232+3G > T, and c.232+1G > T variants [p.(Gly25_Glu77del)] and the p.(Met1?) variants [p.(Trp2_Met103del)] should also disrupt this region of the protein while leaving downstream domains intact (Figure 1D). Although there are no conserved protein motifs in this region, we hypothesize that it harbors an important functional domain necessary for the proper function of CEP85L.

Affected Individuals Have LIS with Variable Developmental Delay and Intractable Seizures

The LIS spectrum includes agyria (sulci, >3 cm apart), pachygyria (sulci, 1.5–3 cm apart), and SBH (Di Donato et al., 2017). Two individuals with a *CEP85L* variant had agyria (with abrupt transition to mild pachygyria anteriorly), two had pachygyria, and the remaining nine had SBH (Table 1). In all 12 individuals where magnetic resonance imaging (MRI) was available for review, LIS was consistently posterior predominant (Figure 1).

Development was variable, ranging from normal (4/13), to mild (3/13), moderate (5/13), and severe (1/13) intellectual disability (ID), with at least one individual attending college (Table

1; intelligence quotient [IQ] scores for four individuals, 58–84). Most individuals could walk (12/13) and all acquired language (13/13), although early language delay occurred in 6 individuals (first words spoken between 18 months and 4 years). At the mild end of the spectrum, two families (V and VIII) presented with autosomal dominant inheritance of SBH with seizures; strikingly there are at least 5 affected individuals over 3 generations in family V. This is in marked contrast to *LIS1*-related posterior predominant LIS that is associated with much more severe neurodevelopmental outcomes.

Epilepsy was present in 12/13 (92%) individuals, with seizure onset ranging from 15 months to 14 years (median, 5 years). Seizures were intractable in all but three individuals. In some (e.g., individual III), normal early development was followed by developmental regression with refractory epilepsy, suggesting that cognitive decline was due to poorly controlled seizures, in addition to the underlying impact of the lesion.

Knockdown of Cep85l Disrupts Normal Neuronal Migration in Mice

LIS spectrum disorders arise due to defects in neuronal migration, resulting in the mislocalization of neurons in the neocortex (Moon and Wynshaw-Boris, 2013). During neocortical development, newly differentiating neurons originate in the ventricular zone (VZ) and medial ganglionic eminence and migrate to their final destination in the neuronal layers of the cortical plate. To determine if disruption of CEP85L results in neuronal migration defects, we used RNA interference (RNAi) to knock down *Cep85l* expression and examine its effect on cortical development. We electroporated either short hairpin RNA (shRNA) targeting *Cep85l* (shCep85l) or a scrambled sequence (shCtrl) into neural stem cells (i.e., radial glial cells [RGCs]) in the VZ of the mouse neocortex at embryonic day 13.5 (E13.5) by *in utero* electroporation. The brains were collected and sectioned at E17.5 and postnatal day 7 (P7) to examine the location and morphology of the progeny cells derived from electroporated RGCs (Figures 2 and S4). At E17.5, most of the GFP^+ cells electroporated with shCtrl (61.47% ± 2.48%, n = 3 animals) had migrated to the cortical plate. However, in the brains electroporated with shCep85l, there were significantly fewer (42.17% ± 2.69%) GFP^+ cells found in the cortical plate (n = 3 mice). Instead, many GFP^+ cells electroporated with shCep85l were found in the intermediate zone (IZ; 20.82% ± 3.29%, n = 3 animals) and subventricular zone (SVZ)/VZ (37.01% ± 1.68%, n = 3 animals) (Figure 2A). The mislocalization of neurons in E17.5 mouse brains electroporated with shCep85l was partially rescued by co-delivery of FLAG-tagged *Cep85l* cDNA along with the shRNA (n = 3 mice; Figure 2A). By P7, neuronal migration defects persisted, with the majority of shCep85l-electroporated GFP+ cells trapped in the SVZ/VZ (Figure 2B). Although neurons failed to properly integrate into the neuronal layers of the cortical plate, co-staining with neuronal marker NeuN indicated that neuronal maturation appeared unaffected (Figure 2C). These results indicate that the loss of CEP85L results in neuronal migration abnormalities, similar to other LIS-associated genes in humans.

CEP85L Localizes to the Pericentriolar Region

Although the precise function of CEP85L is unclear, it contains high sequence homology to CEP85, a protein associated with the centrosome and important for centrosome integrity in inter-phase (Chen et al., 2015; Jakobsen et al., 2011). To examine whether CEP85L is a

centrosomal protein, we cloned and expressed FLAG- or hemagglutinin (HA)-tagged CEP85L in U2OS human osteosarcoma cells. CEP85L formed dot-like structures near centrin staining in each cell, indicating CEP85L is a centrosome-associated protein (Figure 3A). The centrosome is organized by a pair of centrioles surrounded by a matrix of pericentriolar material. We co-stained CEP85L with known centrosome markers at different cell-cycle stages to map its subcentrosomal localization. Centrin and SAS6 served as markers for the distal lumen of the centriole and the proximal end of the pro-centriole, respectively. CEP85L signal was near but did not completely co-localize with SAS-6 or centrin in U2OS cells, indicating CEP85L is not a centriolar protein (Figures 3A and 3B). Rather, we observed that at different cell stages CEP85L was organized into a rosette-like structure, suggesting CEP85L is a pericentriolar protein. The localization of CEP85L at the pericentriolar region was further confirmed by co-staining CEP85L with the pericentriolar material marker pericentrin (Figure 3C). To verify that CEP85L localizes to the centrosome in cortical neurons, embryonic mouse brains were co-electroporated with plasmids expressing eGFP and FLAG-tagged *Cep85l* at E13.5. Brain slices were then stained with γ-Tub and FLAG antibodies at E17.5, showing that FLAG-Cep85l is localized to the centrosome in migrating cortical neurons (Figure 3D). Taken together, our data indicate that CEP85L is a centrosome-associated protein localized specifically to the pericentriolar region.

DISCUSSION

Heterozygous variants in *CEP85L* cause posterior predominant LIS, with a spectrum of severity that ranges from SBH to agyria. Imaging in severe cases shows a characteristic abrupt cutoff from agyria in the occipital, temporal, and parietal lobes to mild pachygyria in the frontal lobes. In *CEP85L*-associated LIS, intractable epilepsy is common, but intellectual outcomes vary markedly from normal intellect to severe ID. Indeed, outcomes can be mild enough that autosomal dominant inheritance occurs, in contradistinction to individuals with *LIS1*-associated LIS who are severely affected and do not reproduce. In a cohort of 14 individuals with posterior predominant LIS previously screened for pathogenic variants in known genes, we identified 3 (21%) unrelated individuals with pathogenic *CEP85L* variants, suggesting *CEP85L* is an important cause of previously unexplained posterior predominant LIS.

The specific pathogenic mechanism leading to *CEP85L*-related disease is unclear. The *CEP85L* gene as a whole is tolerant to loss of function and to missense variation. However, the 4 missense variants that we identified affect a 15-aa region of the protein that is highly intolerant to missense variation, and both the splicing and start-loss variants are predicted to produce a shortened protein that excludes the same 15-aa region. This suggests that the highly constrained region serves an essential function, such as protein-protein binding. Although RNA-seq and western blot data suggest that the splicing and start-loss alleles may be less stable, low levels of abnormal protein are still detectable. Because truncating variants in CEP85L are found in healthy controls, it is unlikely that a simple haploinsufficient model explains the pathogenicity of these heterozygous variants. Instead, pathogenicity appears to result from disruption of the 15-aa constrained region, perhaps through a dominant-negative model. Additional studies are required to determine a specific mechanism.

CEP85L is localized to the centrosome and is an essential protein for neuronal cell migration. Although the majority of genes implicated in LIS spectrum are associated with microtubular dysfunction, a subset of these proteins, including LIS1, are also localized to the centrosome. Individuals with variants in *LIS1* have posterior predominant classical agyria/pachygyria or partial SBH (Di Donato et al., 2018), similar to our cohort, but with a less abrupt cutoff between anterior and posterior brain regions. Loss of *LIS1* results in decoupling of the nucleus from the centrosome and inhibition of inter-nuclear kinesis during neuronal migration (Tanaka et al., 2004). CEP85L and LIS1 both localize to the centrosome, and pathogenic variants in either gene result in abnormal neuronal migration limited primarily to the posterior cortex. This suggests a potential shared disease mechanism, with regional dependence for both LIS1 and CEP85L in the posterior cortex to ensure normal cortical development.

STAR★METHODS

KEY RESOURCES TABLE LEAD CONTACT AND MATERIALS AVAILABILITY

All unique/stable reagents and data generated in this study are available from the Lead Contact with a completed Materials Transfer Agreement. Information and requests for resources and reagents should be directed to, and will be fulfilled by the Lead Contact, Jin-Wu Tsai, PhD (tsaijw@ym.edu.tw).

EXPERIMENTAL MODEL AND SUBJECT DETAILS

Families and Subjects—Affected individuals were identified through clinical practice. Local human research ethics committees approved this study. Written informed consent was obtained from all participants or their parents or legal guardians in the case of minors or those with intellectual disability. Pathogenic variants were identified on a research basis through genome sequencing (Individual I), and exome sequencing (Individuals III, IV, VII IX-a and IX-b). Additional disease-causing variants were identified through targeted sequencing of a cohort of 27 unrelated individuals (31 individuals total) with SBH for whom prior genetics testing including *LIS1* had not identified a genetic etiology (Family V, Individual VI, and Family VIII). Where parental DNA was available, *de novo* status of variants and parental relationships were confirmed. All variants were not present in the genome Aggregation Database (gnomAD v2.1.1).

Animal models—The pregnant ICR mice (BioLASCO) for in utero electroporation are maintained according to the guidelines approved by the Institutional Animal Care and Use Committee (IACUC) at National Yang-Ming University.

METHOD DETAILS

Variant identification and filtering—Pathogenic variants were identified on a research basis through genome sequencing (Individual I), exome sequencing (Individuals III, IV, VII IX-a and IX-b) or targeted sequencing of CEP85L (Individuals V, VI, VIII). Trio genome sequencing was performed using Illumina HiSeq platform (Family I); reads were mapped to hg19 using BWA-MEM (Li and Durbin, 2009) and called with GATK pipeline (DePristo et al., 2011). The variants were filtered for *de novo* inheritance and limited to exon/splice site,

non-synonymous and not present in control databases (gnomAD, ExAC, EVS and TPG). Candidate variants were confirmed by Sanger sequencing.

For individual III, trio exome sequencing was performed by University of Washington Center for Mendelian Genomics (UW-CMG). The exome was captured using the NimbleGen SeqCap EZ Exome v3.0 (Roche) and sequenced on an Illumina Hiseq platform (Illumina, Inc. San Diego, CA. USA) with 75 bp paired-end reads. Sequence reads were aligned to the GRCh37/hg19 reference genome using Burrows-Wheeler Aligner (BWA v0.7.8). Variants were called by the Genome Analysis Toolkit unified genotyper (GATK v3.1.1) and annotated with SeattleSeq (v138) (Ng et al., 2009). Variants not predicted to impact protein coding sequence (synonymous, UTR, or located > 5 bp into the intron) or present (AC > 3) in genome Aggregation Database (v2.1.1) were excluded from further analysis.

Individual IV underwent singleton exome sequencing using the SureSelect QXT CRE platform (Agilent Technologies) with a target mean coverage of 100x; exome data was investigated specifically for variants in *CEP85L* given the phenotypic similarity to the other affected individuals in this series.

Individual VII underwent singleton exome sequencing using the Agilent Clinical Research Exome V2 and an Illumina NovaSeq platform. The reads were mapped to human reference genome (hg19) with BWA and called by Freebayes using the Galaxy platform. Variants were annotated using wANNOVAR and filtered for located in exon or splicing, not in gnomAD, ExAC or 1000GP and not synonymous and CADD score greater than 20 (missense variants only). None of the variants that passed filtering (n = 34) affect reported lissencephaly genes; a variant in *CEP85L* was the best candidate. *De novo* status of the *CEP85L* variant was confirmed via Sanger sequencing of the individual and her parents.

For Family IX, paired end reads were mapped to the human genome hg19 using BWA-MEM; GATK was used to realign reads around known indels, and recalibrate quality scores to reduce artifacts caused by the sequencing chemistry; Picard was used to mark duplicate reads. Variants were identified using haplotype caller within GATK and Freebayes. The intersection of the two variant callers were annotated with SnpEff and loaded into a database using the GEMINI framework. Variants were filtered to identify rare variants (MAF < 0.01) predicted to have a high impact and to be *de novo*.

Additional disease-causing variants (Families V, VI, VIII) were identified through targeted sequencing of a cohort of 27 unrelated individuals (31 individuals total) with SBH for whom prior genetics testing including *LIS1* had not identified a genetic etiology (Family V, Individual VI, and Family VIII). Targeted sequencing was preformed using single molecule molecular inversion probes (smMIPs) (Hiatt et al., 2013) as previously described. Where parental DNA was available, *de novo* status of variants and parental relationships were confirmed. All variants were not present in the genome Aggregation Database (gnomAD v2.1.1).

in utero electroporation—Pregnant ICR mice were used for the *in utero* electroporation (IUE) at E13.5. The procedure for IUE was as previously described (Lu et al., 2018), and followed the approved protocol with the Rodent Survival Surgery Guidelines and Affidavit by the Institutional Animal Care and Use Committee (IACUC) of National Yang-Ming University (NYMU). Briefly, after 2% isoflurane anesthetization, an abdominal incision was made so that the underlying viscera could be exposed. ~1 μL plasmid in TE buffer was injected into the lateral ventricle of each embryonic mouse brain at 3 μg/μl concentration. Electroporation was performed with forceps electrodes (5 mm in diameter) and an electroporation generator (Harvard Apparatus) gave five electric pulses at 40V for 50 ms at 450-ms intervals that transmitted through the uterine wall. After the electroporation, the uterine horns were placed back into the abdominal cavity and the incision was closed by suture. Brains of the electroporated embryos were harvested after the electroporation at E17.5 or P7 for experiments.

RNA-sequencing—RNA was extracted using Trizol (Invitrogen) and RNA Clean and Concentrator (Zymo Research). RNA sequencing library preparation was performed following the manufacturer's instructions using the TruSeq RNA Library Prep Kit v2 (Illumina), which captures non-strand-specific messenger RNA (mRNA) libraries via poly-A selection. Paired-end 100-bp sequencing was performed on an Illumina HiSeq 4000 with targeted sequencing coverage of 50 M reads. Raw reads were mapped to the human genome (GRCh37/UCSC hg19) using STAR (v.2.2.1).

Individual IX-a, IX-b, and control RNA was reverse transcribed following the manufacturer's instructions using oligo(dT) nucleotides and SuperScript II (Invitrogen). Polymerase chain reaction (PCR) to verify splicing defects was performed using primers designed to amplify regions of *CEP85L* encompassing exons 1–3 (Fwd: 5′-AGCCGTTAACCAGCCATCC −3′; Rev: 5′- GCATCACATGGGCAGTAGGA −3′). GAPDH was used as a loading control.

Lymphoblastoid cell lines—In order to study the alteration of translation initiation codon variant p.(Met1?) on the translation of CEP85L, we obtained Epstein-Barr virus transformed lymphoblastoid cell line from Individual I at the Food Industry Research and Development Institute, Taiwan. IM9 lymphoblastoid cell line from the same laboratory was used as control. Cell lines were cultured with RPMI medium and 20% fetal bovine serum. Proteins were harvested from lymphoblastoid cells and analyzed by western blot using anti-C6orf204 (CEP85L) and anti-actin antibodies (Proteintech, USA).

Cep85l knockdown assay—To achieve RNA interference (RNAi)-mediated *Cep85l* knockdown, short hairpin RNA (shRNA) constructs for *Cep85l* based on the pLKO.1-puro or pLKO/U6-TRC011 vector was purchased from the National RNAi Core Facility (Academia Sinica, Taiwan). The *Cep85l* target sequences are listed below: shCep85l-A (5′-TCCAT CTAAC CATCG AAATAA-3′); shCep85l-B (5′-GCATC TACTG AGAAA GAAGTT-3′). These target sequences are conserved between human and mouse. A scrambled sequence (5′-CCTAA GGTTA AGTCG CCCTCG-3′) was used as the control (shCtrl).

Mouse cortical neurons were harvested from E14.5 ICR mouse brains, dissociated with HBSS medium, and placed in papain (20 unit/ml) with HBSS at 37°C for 30 min. Cells were then centrifuged at 1000 × g for 5 min, resuspended with Neuronal basal medium (Life Technologies, USA), B27 (Life Technologies, USA), GlutaMax (GIBCO), penicillin and streptomycin, supplemented with DNase and albumin-ovomucoid inhibitor. The culture dishes were coated with 1% (w/v) poly-D-lysine and 5% Matrigel in artificial cerebrospinal fluid (ACSF) medium at room temperature overnight. Cortical neurons were seeded at 1.25 × 10^6 cells and infected with virus encoding shCep85l-A, shCep85l-B, or shCtrl after 3 days *in vitro* (DIV) for 24 h. Infected neurons were then collected at DIV8 for the detection of Cep85l protein levels by western blot.

CEP85L constructs and site-directed mutagenesis—Mouse *Cep85l* (NM_001204983) and human *CEP85L* (NM_001042475) full-length cDNA based on pcDNA3.1$^+$/C-DYK vector for rescue experiments were purchased from the GenScript. To generate HA-tagged CEP85L, the human *CEP85L* full-length cDNA was amplified by PCR and cloned into pcDNA3-HA vector. The pcDNA3-HA vector was derived from pcDNA3 (Thermo Fisher Scientific) but contained sequences for HA epitope tag between the HindIII and BamHI cloning sites. The mutagenesis PCR protocol was performed following the manufacturer's instructions using QuikChange II Site-Directed Mutagenesis Kit (Agilent Technologies, Cat. #: 200524). The primers used to create CEP85L mutants were: *CEP85L*:c.2T > C: 5′- CCGAG CTCGG ATCCG CCACC ACGTG GGGGC GCTTC CTGGC −3′ (forward) and 5′- GCCAG GAAGC GCCCC CACGT GGTGG CGGAT CCGAG CTCGG −3′ (reverse).

Brain sectioning—Electroporated mouse embryos were perfused transcardially using warm sucrose/phosphate-buffered saline (PBS, pH7.4) followed by cold 4% paraformaldehyde (PFA) in PBS. We collected the brains and post-fixed them in 4% PFA at 4°C overnight. To prepare brains for sectioning, we embedded the brains in 4% low-melting-point agarose dissolved in artificial cerebrospinal fluid (ACSF). Then, the brains were sectioned at a thickness of 100 μm using a Vibratome (Leica, Germany) in the PBS with 0.05% sodium azide (Sigma) at 4°C.

Immunofluorescence—Brain slices were post-fixed in PFA for 20 min at room temperature (RT), followed by blocking at RT for 1 h with 10% NGS, 5% BSA and 0.2% Triton X-100 in PBS. Primary antibodies were then applied and incubated two days at 4°C at the following concentrations: anti-Cep85l rabbit polyclonal antibody (1:1000 for cells, 1:200 for slices, Proteintech, Cat. #: 24588–1-AP); anti-γ-Tub rabbit polyclonal antibody (1:500, Abcam, Cat. #: ab11317); anti-GFP chicken polyclonal antibody (1:1000, Abcam, Cat. #: ab13970); anti-NeuN rabbit polyclonal antibody (Millipore, 1:500). Slices were washed with PBS and incubated in Alexa Fluor 488-/ Alexa Fluor 546-/ Alexa Fluor 647-conjugated secondary antibodies (1:500, Invitrogen) at RT for 2 h. DNA was stained with 4',6-diamidino-2-phenylindole (DAPI) (Molecular Probes). Confocal images were acquired using Zeiss LSM700 confocal microscope and analyzed by ZEN software (Zeiss) and ImageJ (NIH).

Cell culture and transfection—HEK293T (human embryonic kidney cells) and U2OS (human osteosarcoma) cell lines were cultured in Dulbecco's Modified Eagle Medium (DMEM, Life Technologies, USA) supplemented with 10% fetal bovine serum, 1% L-glutamine and 1% penicillin/streptomycin. To carry out the transfection, we plated NIH 3T3 cells on 60 mm dishes at 70%–80% confluency, transfected with the Lipofectamine 2000 and P3000 lipofection reagents (Life Technologies, USA) according to manufacturer's protocol, and harvested cells 24 h later. Transient transfections of U2OS cells were performed using T-Pro NTR II transfection reagents (T-Pro Biotechnology). 1×10^6 of cells were plated on 60-mm plate for overnight. Cells were transfected with 4 μg of expression constructs according to the manufacturer's instructions and harvested 48 h after transfection.

Centrosome staining and imaging—Cells were grown on coverslip coated with 0.1 mg/ml of poly-L-lysine and fixed with methanol at −20°C for 15 min. Cells were then incubated in the blocking buffer that contained 3% bovine serum albumin (w/v) and 0.1% Triton X-100 in PBS for 30 min at RT. Primary antibodies were all diluted in blocking buffer and incubated for 2 h at RT. Primary antibodies were obtained from the following sources and used according to the manufacturers' instructions: mouse anti-centrin (1:1,000; 04–1624; Millipore), mouse anti-HA (1:1000; 901503; BioLegend), mouse-anti-Flag (1:1,000; F3165; Sigma-Aldrich), mouse anti-SAS6 (1:250; sc-81431; Santa Cruz), and rabbit anti-perincentrin (1:2,000; 4448; Abcam). Alexa Fluor 488–, 594–, or 680-conjugated goat secondary antibodies were used at 1:500 dilution (Molecular probes) and incubated for 1 h at RT. DNA was visualized using 4', 6-diamidino-2-phenylindole (DAPI; Thermo Fisher Scientific). Fluorescent images were obtained using an upright microscope (Axio imager. M2 ApoTome2 sysyem; Carl Zeiss) with a Plan-NEOFLUAR × 100 (1.3 NA) oil-immersion objective and a Axiocam 702 CCD camera. Images were acquired and processed by ZEN software (Carl Zeiss).

Electrophoresis and western blotting—Transfected or infected cells were lysed in RIPA buffer (50mM Tris-HCl, pH 8.0, 150mM NaCl, 1% Nonidet P-40, 0.5% sodium deoxycholate, 0.1% SDS) with protease inhibitor and phosphatase inhibitor (Sigma Aldrich). Protein concentration of cell or cortex lysates were determined by Pierce BCA Protein Assay Kit (Thermo Fisher Scientific, Cat. #: 23225). Protein samples (30–40 μg/lane) were separated on a 10% SDS polyacrylamide gel electrophoresis (SDS-PAGE) with a constant voltage of 100V. Samples were then transferred to polyvinylidene difluoride (PVDF) membrane (Millipore) using a transfer apparatus (Bio-red) filled with transfer buffer including 15% methanol. After a two-hour transfer at 100V, the PVDF membranes were incubated in 5% skim milk in TBST buffer (TBS buffer with 0.1% Tween-20) at RT for 1 h, followed by the primary antibody incubation overnight at 4°C. The primary antibodies used were: anti-Cep85l rabbit polyclonal antibody (1:50000, Proteintech, Cat. #: 24588–1-AP); anti-FLAG (DYKDDDDK) mouse monoclonal antibody (1:10000, GenScript, Cat. #: A00187–100), anti-GAPDH mouse monoclonal antibody (1:10000 Proteintech, Cat. #: 60004–1-Ig), anti-β-actin mouse monoclonal antibody (1:10000 Proteintech, Cat. #: 66009–1-Ig). The immunoblots were washed three times in TBST, 10 min for each time, and then immersed in secondary antibody solution containing goat anti-mouse IgG-HRP (1:10000, Millipore) or goat anti-rabbit IgG-HRP (1:10000, Sigma-Aldrich) at RT for 2 h. The

immunoblots were visualized using an immobilon western chemiluminescent HRP substrate (Millipore) and quantified by Fujifilm LAS-4000 chemiluminescence detection system.

QUANTIFICATION AND STATISTICAL ANALYSIS

All data are expressed as mean ± SD. Student's t tests were used to compare differences between two experimental conditions unless otherwise noted. All statistical tests were two sided. Statistical significance was set at $p < 0.05$ (95% confidence level). For all experiments, $n \geq 3$ animals were analyzed for each group.

DATA AND CODE AVAILABILITY

The human sequence data supporting the current study have not been deposited in a public repository due to reason of individual consent. Please contact the author with individual requests.

ADDITIONAL RESOURCES

Detailed clinical histories for affected individuals.

Individual I—Pachygryria, posterior predominant

CEP85L: p.(Met1?): This 20-year-old Taiwanese man had posterior predominant pachygyria with moderate intellectual disability and epilepsy. He was born by elective Caesarean section. He had delayed speech milestones, acquiring single words at 18 months of age. He required educational assistance throughout his education. He had two febrile seizures at 3 and 4 years, each lasting for about 5 minutes. Epilepsy was diagnosed at 8 years of age when he developed focal impaired awareness seizures characterized by motor arrest, loss of awareness, and sometimes orolingual and ambulatory automatisms. His seizures were precipitated by fever, upper respiratory tract infection and sleep deprivation and tended to occur in the early morning. There were no myoclonic or tonic seizures. Seizures occurred about 1–2 times per month despite multiple anti-epileptic drugs. A vagal nerve stimulator was implanted at age 16 years but was not beneficial. His EEG showed bilateral occipital epileptiform discharges. He also had hypodontia of his permanent teeth. There was no family history of epilepsy or learning difficulties.

Individual II—Pachygryria

CEP85L: p.(Met1?): This individual was ascertained through a literature search from exome sequencing by the Deciphering Developmental Disorders study as noted in the main text. Limited phenotypic information is available.

Individual III—SBH, posterior predominant

CEP85L: p.(Ser58Cys): This 52-year-old male had normal early development; he walked and talked before his siblings. At age 3.5 years there was an explosive onset of absence, atonic and tonic seizures. EEGs showed very frequent slow spike-and-wave discharges and paroxysmal fast activity. The electro-clinical diagnosis was Lennox-Gastaut syndrome.

Intellectual slowing was noted at age 4 years and he required special schooling from age 5 due to very frequent seizures but also regression. Seizures proved intractable despite multiple medications. He was able to run until age 20 when he became more clumsy. He had moderate intellectual disability being able to recognize some words but not read. Despite ongoing seizures in middle age, he retained good social and language skills but seizures continued with frequent falls requiring a helmet.

Individual IV—Agyria posteriorly, with abrupt transition to pachygyria anteriorly

CEP85L: p.(Asp65Asn): This 3-year old male, the first-born child in his family, was the product of a normal pregnancy and delivery. There was no relevant family history. He had motor feeding difficulties after birth and delayed gross motor milestones identified by 6 months of age, resulting in medical review and MRI was performed. Left torticollis was present in infancy. He developed seizures at age 15 months, with multiple daily events of sudden sustained head drop with eye deviation to either side or upward, sometimes with brief upper body tonic stiffening. Interictal awake EEG showed an abnormal background dominated by beta frequencies with amplitude increasing posteriorly and relatively frequent sharp and slow waves over posterior regions independently bilaterally. Interictal spasm complexes were present, but no ictal correlate to the head drops was recorded. No developmental regression occurred at the time of seizure onset, however global developmental impairment was evident by 18 months of age. At age 3 years he can crawl and cruise but cannot stand or walk without support. He uses approximately five single words. His neurological examination shows hypotonia and brisk reflexes in lower limbs, resulting in a clinical diagnosis of GMCSF II cerebral palsy. He requires glycopyrrolate for excessive drooling. He has no dysmorphic features. Seizures are controlled with Valproate monotherapy.

Individual V-a—SBH, thin posterior

CEP85L: p.(Ile68Thr): This woman had onset of seizures at 12 years, consisting of both GTCS and focal impaired awareness seizures involving prolonged disorientation with nonpurposeful behaviors that were intractable to phenytoin and phenobarbital. She attended regular school and some college courses. Her later history was significant for multiple psychiatric hospitalizations with reports of depression, auditory hallucinations and suicide attempts. She passed away at 52 years of age from lung cancer. Family history is notable for three similarly affected sons (Individual V-b, V-c V-d) and a similarly affected grandson (Individual V-e).

Individual V-b—SBH, posterior predominant

CEP85L: p.(Ile68Thr): This 35-year-old man had onset of GTCS preceded by confusion or visual changes at 14 years, but may have also had febrile seizures in infancy. EEGs showed single diffuse spike-wave complexes and slow background. His seizures were intractable to phenytoin, valproate, carbamazepine, zonisamide, levetiracetam, and rufinamide. His early development was normal, but he later attended Special Education classes and did not

graduate high school. He had a history of aggressive behavior and suicide attempts and was diagnosed with bipolar disorder.

Individual V-c—SBH, posterior predominant

CEP85L: p.(Ile68Thr): This 47-year-old man had onset of GTCS with focal onset and aura consisting of hand tingling at 12 years. Seizures were intractable to phenytoin, zonisamide, and levetiracetam. His EEG at 44-years-old detected frequent sharp waves over the parietal region. His early development was normal but he attended special education classes and was unable to read or write as an adult. He had problems with aggressive behavior and substance abuse. Family history is notable for similarly affected son (Individual V-e).

Individual V-e—Pachygyria with SBH, posterior predominant

DNA unavailable: This 26-year-old man had onset of GTCS at 16 years that were controlled with levetiracetam. EEG showed right parietal spike discharges. His early development was normal but he attended an alternative school due to aggressive behavior and dropped out in the 10th grade. Brain MRI showed pachygyria and bilateral bands of SBH beginning posterior to the precentral sulcus and throughout the parietal cortex.

Individual VI—SBH, posterior predominant

CEP85L: p.(Glu69Arg): This 22-yo woman presented with mild delays in the first year of life and with absence seizures at 4 years of age. She soon developed atonic seizures. She continues to have atonic and absence seizures daily, with longer seizures approximately three times per week that are intractable to medication.

Individual VII

NM_001042475.1: c.232+1G > T: This 25-year-old female presented with seizure at 5 months old. Her seizure types include tonic, myoclonic and atonic seizures. She had 4 seizures before 6 years of age; from age 6, her seizures have been intractable. She has moderate global developmental delay with speech onset at 4 years old. Her EEG showed interictal multifocal and generalized sharp waves, generalized paroxysmal fast activities, and ictal decremental response. MRI brain showed posterior lissencephaly with pachygyria.

Individual VIII-a—SBH, posterior predominant

NM_001042475.1: c.232+3G > T: This 30-year-old man had onset of focal impaired awareness seizures at 12 years, characterized by unconsciousness and abnormal gait with discoordinated and slow movements. No EEG data was available. His seizures were controlled by medication. He has borderline cognitive function. He has visual agnosia and somatognosia disturbances with spared praxic skills. Family history is notable for a similarly affected daughter (Individual VIII-b). The clinical details for this individual were previously published as noted in the main text.

Individual VIII-b—SBH, posterior predominant

NM_001042475.1: c.232+3G > T: This 5-year-old girl has focal impaired awareness and generalized seizures, controlled by medication (valproate). No EEG data was available. Early development was normal. She has borderline cognitive function and slight language delay and mild microcephaly (−2SD). Family history is notable for a similarly affected father (Individual VIII-a). The clinical details for this individual were previously published as noted in the main text.

Individual IX-a—SBH, posterior predominant

NM_001042475.1: c.232+5G > A: This 21-year-old female has intractable epilepsy, borderline intellectual functioning (full-scale IQ 69). Her developmental history is significant for speech delay, with first words at 3.5 years; she continues to have challenges with initiating conversation and with accents and tonality but speaks in sentences. Gross motor development was normal. She has Asperger syndrome with features including always fiddling with different things, limited social skills, difficulties and challenges with any changes, being hyper-focused, in addition to a tendency for repetition, spinning behavior and multiple other stereotypies. Seizure onset was at 7 years of age; she has multiple seizure types including generalized tonic-clonic, absence, and focal seizures. She required special education classes for reading; she performed well in math. She has a part-time job at a restaurant, takes the bus by herself and does most self-care independently though requires reminders and some supervision. She has severe myopia. Family history is notable for a similarly affected sister (Individual IX-b). Her mother had absence seizures with onset at age 6 that were treated through age 16, without recurrence since withdrawal of medication; the individual's father has autism spectrum disorder.

Individual IX-b—SBH, posterior predominant

NM_001042475.1: c.232+5G > A: This 19-year-old female has intractable epilepsy, mild intellectual disability (full-scale IQ 58). She had speech delay with first words at 4 years old and approximately 20 words at 5 years. Her speech has improved over time but remains immature, and she requires help with creating multi-syllable words, for example. In school, she required special education classes with occasional mainstream classes with accommodation. Seizures began at 6 years and include absence and focal seizures; she has never been seizure free. She has mild myopia. Family history is notable for a similarly affected sister. Her mother had absence seizures with onset at age 6 that were treated through age 16, without recurrence since withdrawal of medication; the individual's father has autism spectrum disorder.

Supplementary Material

Refer to Web version on PubMed Central for supplementary material.

ACKNOWLEDGMENTS

We thank the patients and their families for participating in this study. We thank Dr. Sarah Barton for assistance with MRI image processing. This work was supported by the University of Washington Birth Defects Research Laboratory (NIH 5R24HD000836) and the University of Washington Intellectual and Developmental Disabilities

Research Center (IDDRC; NIH U54HD083091) from the Eunice Kennedy Shriver National Institute of Child Health and Human Development. Sequencing was provided by the University of Washington Center for Mendelian Genomics (UW-CMG) and was funded by NHGRI and NHLBI grants UM1 HG006493 and U24 HG008956. The content is solely the responsibility of the authors and does not necessarily represent the official views of the National Institutes of Health. A.M.M. received support from the American Epilepsy Society. H.C.M. received support from the National Institutes of Health (NIH R01 NS069605). M.-H.T. received support from Chang Gung Medical Foundation (CGMF grant CMRPG8G0252), Whole-Genome Research Core Laboratory of Human Diseases at CGMF, and Ministry of Science and Technology (MOST grants 106-2314-B-182A-077 and 107-2314-B-182A-057-MY3), Taiwan. J.-W.T. received support from MOST (103-2628-B-010-002-MY3, 106-2628-B-010-002-MY3, 107-2633-B-009-003, 107-2221-E-010-014, 108-2638-B-010-001-MY2, and 108-2321-B-010-011-MY2), the National Health Research Institute (NHRI), the Brain Research Center, NYMU through the Featured Areas Research Center Program within the framework of the Higher Education Sprout Project by the Ministry of Education, and NYMU School of Medicine (107F-M01-0502), Taiwan. W.-J.W. received support from MOST (108-2628-B-010-007 and 107-2313-B-010-001). G.M.M. received support from the National Institute of Neurological Disorders and Stroke (NINDS) under award number K08NS092898, Jordan's Guardian Angels, and the Brotman Baty Institute. I.E.S. and S.F.B. were supported by National Health and Medical Research Council (NHMRC) of Australia (program grant 628952, 2011–2015; 1091593, 2016–2020); I.E.S. has a NHMRC Senior Practitioner Fellowship (1006110, 2011–2015; 1104831 2016–2020). M.S.H. was supported by a NHMRC Career Development Fellowship (1063799) and project grant (1079058). R.J.L. is supported by a Melbourne Children's Clinician Scientist Fellowship. Support was received from the Australian Genomics Health Alliance, funded by NHMRC grant 1113531 and the Australian Government's Medical Research Future Fund.

REFERENCES

Chen C, Tian F, Lu L, Wang Y, Xiao Z, Yu C, and Yu X (2015). Characterization of Cep85—a new antagonist of Nek2A that is involved in the regulation of centrosome disjunction. J. Cell Sci 128, 3837. [PubMed: 26471995]

Deciphering Developmental Disorders Study. (2017). Prevalence and architecture of *de novo* mutations in developmental disorders. Nature 542, 433–438. [PubMed: 28135719]

Deconinck N, Duprez T, des Portes V, Beldjord C, Ghariani S, Sindic CJ, and Sébire G (2003). Familial bilateral medial parietooccipital band heterotopia not related to DCX or LIS1 gene defects. Neuropediatrics 34, 146–148. [PubMed: 12910438]

DePristo MA, Banks E, Poplin R, Garimella KV, Maguire JR, Hartl C, Philippakis AA, del Angel G, Rivas MA, Hanna M, et al. (2011). A framework for variation discovery and genotyping using next-generation DNA sequencing data. Nat. Genet 43, 491–498. [PubMed: 21478889]

Desmet FO, Hamroun D, Lalande M, Collod-Béroud G, Claustres M, and Béroud C (2009). Human Splicing Finder: an online bioinformatics tool to predict splicing signals. Nucleic Acids Res. 37, e67. [PubMed: 19339519]

Di Donato N, Chiari S, Mirzaa GM, Aldinger K, Parrini E, Olds C, Barkovich AJ, Guerrini R, and Dobyns WB (2017). Lissencephaly: Expanded imaging and clinical classification. Am. J. Med. Genet. A 173, 1473–1488. [PubMed: 28440899]

Di Donato N, Timms AE, Aldinger KA, Mirzaa GM, Bennett JT, Collins S, Olds C, Mei D, Chiari S, Carvill G, et al.; University of Washington Center for Mendelian Genomics (2018). Analysis of 17 genes detects mutations in 81% of 811 patients with lissencephaly. Genet. Med 20, 1354–1364. [PubMed: 29671837]

Dobin A, Davis CA, Schlesinger F, Drenkow J, Zaleski C, Jha S, Batut P, Chaisson M, and Gingeras TR (2013). STAR: ultrafast universal RNA-seq aligner. Bioinformatics 29, 15–21. [PubMed: 23104886]

Havrilla JM, Pedersen BS, Layer RM, and Quinlan AR (2019). A map of constrained coding regions in the human genome. Nat. Genet 51, 88–95. [PubMed: 30531870]

Hiatt JB, Pritchard CC, Salipante SJ, O'Roak BJ, and Shendure J (2013). Single molecule molecular inversion probes for targeted, high-accuracy detection of low-frequency variation. Genome Res. 23, 843–854. [PubMed: 23382536]

Jakobsen L, Vanselow K, Skogs M, Toyoda Y, Lundberg E, Poser I, Falkenby LG, Bennetzen M, Westendorf J, Nigg EA, et al. (2011). Novel asymmetrically localizing components of human centrosomes identified by complementary proteomics methods. EMBO J. 30, 1520–1535. [PubMed: 21399614]

Lek M, Karczewski KJ, Minikel EV, Samocha KE, Banks E, Fennell T, O'Donnell-Luria AH, Ware JS, Hill AJ, Cummings BB, et al.; Exome Aggregation Consortium (2016). Analysis of protein-coding genetic variation in 60,706 humans. Nature 536, 285–291. [PubMed: 27535533]

Li H, and Durbin R (2009). Fast and accurate short read alignment with Burrows-Wheeler transform. Bioinformatics 25, 1754–1760. [PubMed: 19451168]

Lu IL, Chen C, Tung CY, Chen HH, Pan JP, Chang CH, Cheng JS, Chen YA, Wang CH, Huang CW, et al. (2018). Identification of genes associated with cortical malformation using a transposon-mediated somatic mutagenesis screen in mice. Nat. Commun 9, 2498. [PubMed: 29950674]

Moon HM, and Wynshaw-Boris A (2013). Cytoskeleton in action: lissencephaly, a neuronal migration disorder. Wiley Interdiscip. Rev. Dev. Biol 2, 229–245. [PubMed: 23495356]

Myers CT, Hollingsworth G, Muir AM, Schneider AL, Thuesmunn Z, Knupp A, King C, Lacroix A, Mehaffey MG, Berkovic SF, et al. (2018). Parental Mosaicism in "De Novo" Epileptic Encephalopathies. N. Engl. J. Med 378, 1646–1648. [PubMed: 29694806]

Ng SB, Turner EH, Robertson PD, Flygare SD, Bigham AW, Lee C, Shaffer T, Wong M, Bhattacharjee A, Eichler EE, et al. (2009). Targeted capture and massively parallel sequencing of 12 human exomes. Nature 461, 272–276. [PubMed: 19684571]

Tanaka T, Serneo FF, Higgins C, Gambello MJ, Wynshaw-Boris A, and Gleeson JG (2004). Lis1 and doublecortin function with dynein to mediate coupling of the nucleus to the centrosome in neuronal migration. J. Cell Biol 165, 709–721. [PubMed: 15173193]

Highlights

- Autosomal dominant variants in *CEP85L* cause posterior predominant lissencephaly
- Intellect ranges from normal to severely affected in *CEP85L*-associated lissencephaly
- CEP85L is a centrosome protein localizing to the pericentriolar material
- Knockdown of *Cep85l* in mouse causes a neuronal migration defect

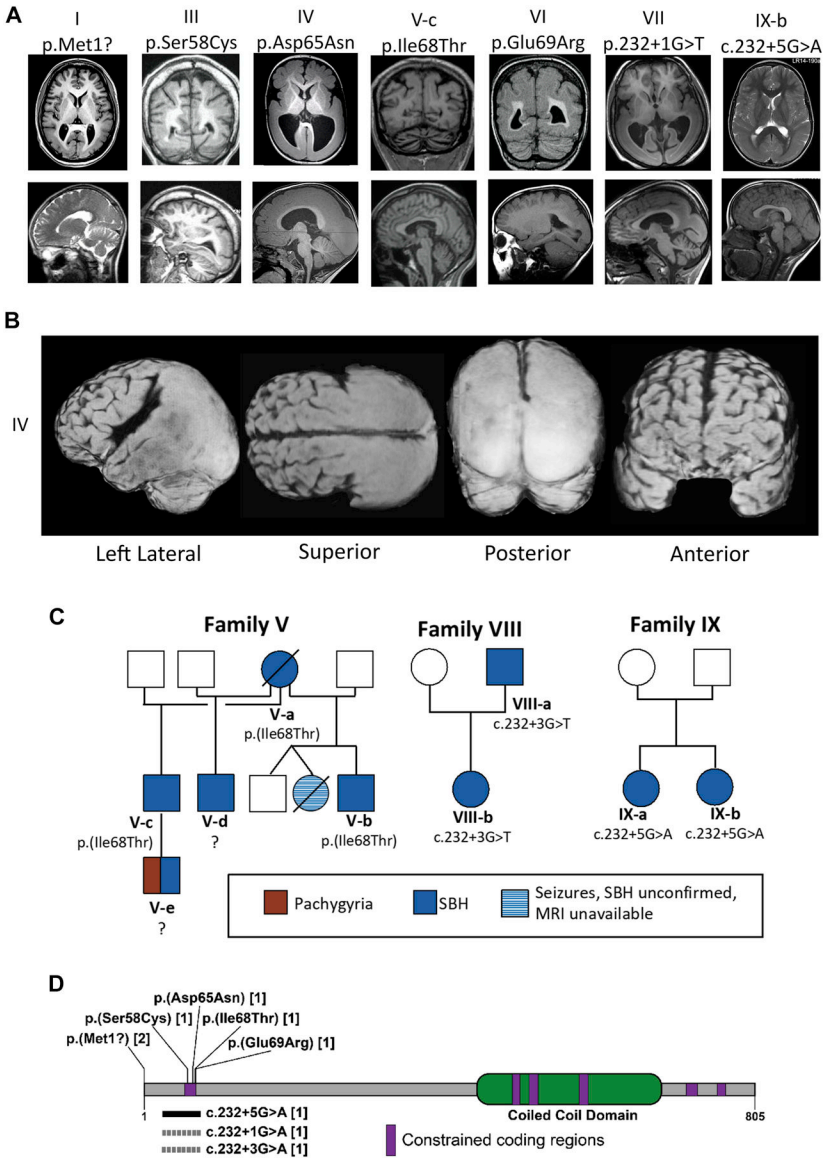

Figure 1. Brain MRIs in Individuals with Heterozygous CEP85L Variants Show Posterior LIS Due to De Novo or Inherited Variants in CEP85L

(A) Selected brain MRI scans of individuals with heterozygous *CEP85L* variants. Individual I shows pachygyria over occipital and parietal regions with mild cerebellar atrophy (axial and sagittal views). Individuals IV and VII showed agyria in the occipital and posterior temporal and parietal lobes with an abrupt transition to mild pachygyria anteriorly. On T2 imaging, prominent intracortical linear high signal was also seen posteriorly consistent with a cell sparse zone, seen here on T1 images as subtle intracortical linear low or mixed signal. Individuals III, V-c, VI, and IX-b show subcortical band heterotopia (SBH or double cortex) over the same posterior distribution (coronal and sagittal views). Images for additional cases are shown in Figure S1.

(B) Three-dimensional surface rendering imaging of individual IV showed the lack of gyration of parietooccipito-temporal region with an abrupt transition to near normal gyration

pattern around the Sylvian fissure and central sulcus. Anterior temporal pole sparing was noted.

(C) Pedigrees of familial lissencephaly show rare heterozygous *CEP85L* variants segregate with disease in family V, VIII, and IX. For family IX, despite targeted deep sequencing, we did not detect mosaicism for the variant in either parent, suggesting the mosaicism was limited to the gonads. Affected individuals for whom DNA is unavailable are indicated by a question mark. SBH, subcortical band heterotopia.

(D) Distribution of disease-causing variants across CEP85L. Missense variants are clustered within a constrained coding region highly intolerant to protein changing variation. Highly constrained coding regions in *CEP85L* (>90th percentile of all coding regions in the genome) are denoted by purple boxes. The black horizontal bar under the schematic represents the deletion due to skipping of exon 2 caused by the c.2323+5G > A variant. The gray dashed bars represent the predicted deletions caused by the c.2323+1G > T and c.2323+3G > T variants. Numbers in brackets indicate the number of unrelated individuals harboring the variant. Variants are annotated using transcript NM_001042475.

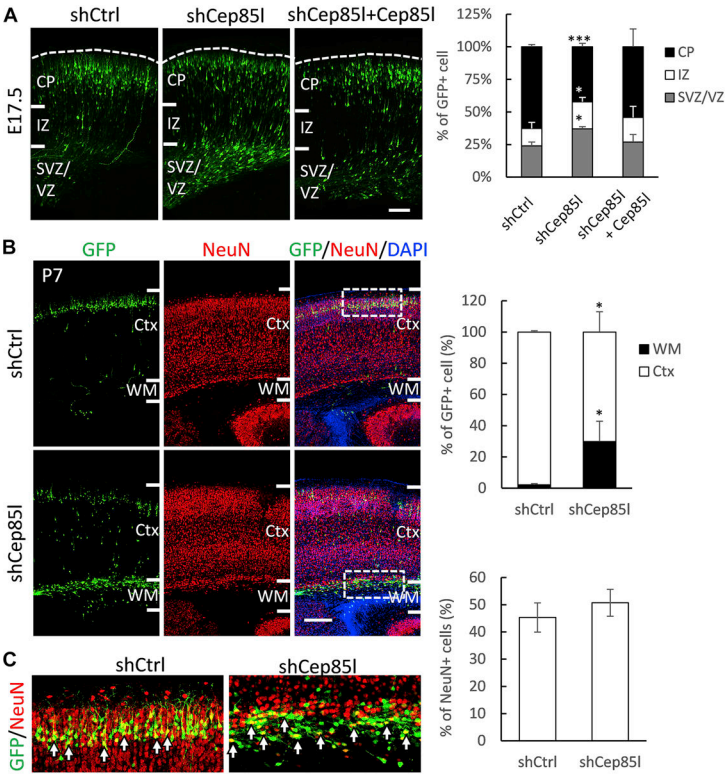

Figure 2. Loss of Cep85l Disrupts Neuronal Migration in the Developing Mouse Cortex but Does Not Interfere with Neuronal Maturation

(A) Representative images of E17.5 coronal sections of mouse cortices electroporated at E13.5 with shCtrl, shCep85l, or shCep85l together with *Cep85l* cDNA. In the control brain electroporated with shCtrl, the majority of transfected cells (labeled with EGFP, green) have migrated to the CP. In contrast, a large portion of cells electroporated with shCep85l remained in the VZ/SVZ and IZ. This altered cell distribution was partially rescued by Cep85l expression. Bar, 100 μm. CP, cortical plate; IZ, intermediate zone; SVZ, subventricular zone; VZ, ventricular zone. Bar graph represents the percentage of GFP+ cells in each region in these conditions. Error bars represent SD. *$p < 0.05$, ***$p < 0.001$ (ANOVA test, n = 3 experiments).

(B) Representative images of P7 coronal sections of mouse cortices electroporated with shCtrl or shCep85l at E13.5. In the control brain electroporated with shCtrl, almost all of transfected GFP+ cells (green) have reached to the cortex marked with the neuronal marker NeuN (red). However, many shCep85l-electroporated cells remained in the white matter and deep layers of the cortex. Brain slices are co-stained with 4′,6-diamidino-2-phenylindole, dihydrochloride (DAPI; blue) for the nuclei. Bar, 200 μm. Ctx, cortex; WM, white matter. Bar graph represents the percentage of GFP+ cells in each region in these conditions. Error bars represent SD. *$p < 0.05$ (Student's t test, n = 3 experiments).

(C) High-magnification images of the boxes in (B) highlighting NeuN expression in GFP+ cells (arrows). Bar graph shows no significant difference in NeuN expression between shCtrl- and shCep85l-electro-potated cells at P7 (Student's t test). Error bars represent SD.

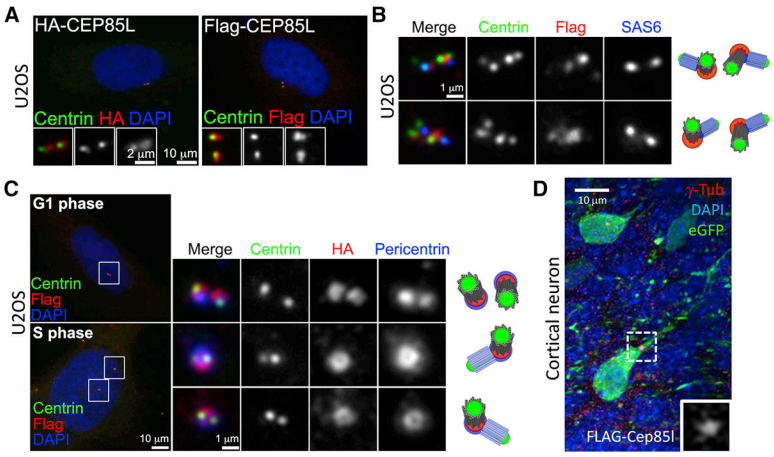

Figure 3. CEP85L Is a Centrosomal Protein

(A) U2OS cells transfected with FLAG- or HA-tagged CEP85L for 48 h were subjected to immunofluorescence staining with centrin (green), FLAG (red), and HA (red) antibodies. Bar, 10 μm for large image, 2 μm for insets.

(B) U2OS cells transiently transfected with FLAG-tagged CEP85L and stained with centrin (green), FLAG (red), and SAS6 (blue) antibodies. Schematic representations of the centrosome association of centrin (green), FLAG-CEP85L (red), and SAS6 (blue) are shown. Bar, 1 μm.

(C) Immunofluorescence images were obtained from U2OS cells transfected with FLAG-tagged CEP85L at various cell-cycle stages. FLAG-tagged CEP85L (red) was localized to pericentrin (PCM marker, blue). Schematic representations of the centrosome association of centurion (green), FLAG-CEP85L (red), and pericentrin (blue) are shown. Bar, 10 μm for large image, 1 μm for insets.

(D) Representative image of a mouse brain electroporated with FLAG-tagged *Cep85l* at E13.5. FLAG-Cep85l (white) was localized to the centrosomal marker γ-tubulin (red) in the leading process of a migrating neuron. All cells were counterstained with DAPI staining (blue) to show the nuclei. Bar, 10 μm.

Table 1.

Phenotypic and Genetic Features of Individuals with CEP85L variants

Individuals	Sex	Variant (hg19) (NM_001042475)	Inheritance	MRI	Seizure onset (age, type)	EEG	Development	Other
I	M	chr6:118972431A > G p.(Met1?)	*De novo*	Pachygryria, posterior predominant	Onset 3 y: febrile seizures; epilepsy at 8 y with myoclonic, tonic, and atonic seizures	Bilateral occipital epileptiform discharges	Language delay (first words 18 m), moderate ID	Hypodontia
II[a]	M	chr6:g.118972432T > A p.(Met1?)	*De novo*	Pachygyria, white matter neuronal heterotopia	Unknown	Unavailable	Mild ID	Cortical visual impairment
III	M	chr6:g.118953676T > A p.(Ser58Cys)	*De novo*	SBH, posterior predominant (parietal, occipital, and temporal lobes)	Onset 3 y 6 m: atonic; atypical absence, tonic, intractable	Slow spike and wave discharges, frequent bursts of generalized paroxysmal fast activity	Normal prior to seizure onset, delay noted by age 4 y, moderate ID	Mild cerebellar impairment Slight dystonic posturing of neck and left hand Gum hypertrophy (phenytoin)
IV	M	chr6:118953655C > T p.(Asp65Asn)	*De novo*	Agyria posteriorly, with abrupt transition to pachygyria anteriorly	Onset 15 m: head drops and eye deviation, well controlled by valproate	Awake background dominated by beta frequencies with amplitude increasing posteriorly. Interictal sharp and slow waves over posterior regions independently. Electrographic spasm complexes present, but no ictal correlate to head drops.	Global delay; at 3y uses ~5 single words, unable to stand or walk without support	Left torticollis
V-a	F	chr6:g.118953645A > G p.(Ile68Thr)	Inheritance unknown	SBH, thin posterior	Onset 12 y: GTC and focal impaired awareness seizures; intractable	Unavailable	Normal; graduated high school, some college	Depression, auditory hallucinations and suicide attempts
V-b	M	chr6:g.118953645A > G p.(Ile68Thr)	Maternally inherited	SBH, posterior predominant (parietal and occipital lobes)	Possible febrile seizure in infancy. Onset 14 y: generalized seizures; intractable	Slow background with isolated single diffuse spike-wave complexes (14 y)	Early development normal; attended special education classes, did not graduate high school	Bipolar disorder, aggressive behavior, suicide attempts
V-c	M	chr6:g.118953645A > G p.(Ile68Thr)	Maternally inherited	SBH, thin posterior	Onset 12 y: GTC with focal onset; intractable	Frequent sharp waves over the parietal region (44 y)	Early development normal; attended special education classes, unable to read and write	Aggressive behavior, substance abuse
VI	F	chr6:g.118953643C > T p.(Glu69Arg)	Inheritance unknown	SBH, posterior predominant	Diagnosed at 4 y: absence, atonic, focal impaired awareness with motor feature; in retrospect seizures	Unavailable	Moderate ID (academic skills are at 2nd-4th grade level); walks and runs slowly, poor fine motor skills	Cortical visual impairment

Individuals	Sex	Variant (hg19) (NM_001042475)	Inheritance	MRI	Seizure onset (age, type)	EEG	Development	Other
					probably at birth or even in utero.			
VII	F	chr6:g.118953615C > A c.232+1G > T	Inheritance unknown	Agyria, posterior predominant	Onset 5 mo: tonic, myoclonic, atonic	Multifocal and generalized sharp and slow waves, GPFA, ictal sharp waves with decremental response	Moderate global delay; first words at 4 y	
VIII-a[b]	M	chr6:g.118953613C > A c.232+3G > T	Inheritance unknown	SBH, posterior predominant (parietal and occipital lobes)	Onset 12 y: focal impaired awareness seizures; controlled by medication	Slow background with superimposed symmetrical bilateral parietooccipital slowing with occasional spikes	Normal (IQ: 82)	Visual agnosia and somatognosia disturbances with spared praxic skills
VIII-b[b]	F	chr6:g.118953613C > A c.232+3G > T	Paternally inherited	SBH, posterior predominant (parietal and occipital lobes)	Onset before 5 y: focal impaired awareness and generalized seizures; controlled by medication (valproate)	Slow background with superimposed symmetrical bilateral parietooccipital slowing with occasional spikes	Normal (IQ: 84); mild language delay	Mild microcephaly (−2 SD)
IX-a	F	chr6:g.118953611C > T c.232+5G > A	*De novo* (parental germline mosaicism suspected)	SBH, posterior predominant	Onset 7 y: focal impaired awareness, absence, GTC; intractable	Unavailable	Normal gross motor, but awkward movements; delayed fine motor and speech; first words 3.5 y; mild ID (IQ 69)	Autism; myopia
IX-b	F	chr6:g.118953611C > T c.232+5G > A	*De novo* (parental germline mosaicism suspected)	SBH, posterior predominant	Onset 6 y: focal impaired awareness; intractable; also has visual disturbances	Multi-focal bilateral spikes; intermittent slow, left occipital; suggestive of focal epilepsy arising from posterior region	Global delay; first words at 4 y; mild ID (IQ 58)	

EEG, electroencephalogram; F, female; GPFA, generalized paroxysmal fast activity; GTC, generalized tonic-clonic seizures; ID, intellectual disability; M, male; m, months; SBH, subcortical band heterotopia; y, years

[a]The genetic information for individual II was previously published as part of the Deciphering Developmental Disorders study (Deciphering Developmental Disorders, 2017). MRI was unavailable for review.

[b]The clinical details for individuals VIII-a and VIII-b were previously published (Deconinck et al., 2003).

KEY RESOURCES TABLE

REAGENT or RESOURCE	SOURCE	IDENTIFIER
Antibodies		
Mouse anti-actin	Proteintech	Cat#: 60008-1; RRID: AB_2289225
Rabbit anti-C6orf204 (CEP85L)	Proteintech	Cat#: 24588-1-AP; RRID: AB_2819012
Rabbit anti-Neun	Millipore	Cat# ABN78; RRID: AB_10807945
Mouse anti-Centrin	Millipore	Cat#: 04-1624; RRID: AB_10563501
Rabbit anti-Pericentrin	Abcam	Cat#: ab4488; RRID: AB_304486
Rabbit anti-gamma Tubulin	Abcam	Cat#: ab11317; RRID: AB_297921
Mouse anti-SAS6	Santa Cruz	Cat#: sc-81431; RRID: AB_1128357
Mouse anti-GAPDH	Proteinch	Cat#: 60004-1-Ig; RRID: AB_2107436
Mouse anti-β-actin	Proteinch	Cat#: 66009-1-Ig; RRID: AB_2687938
Mouse anti-HA	BioLegend	Cat#: 901503; RRID: AB_2565005
Mouse anti-Flag(DYKDDDDK)	GenScript	Cat#: A00187-100; RRID: AB_1720813
Mouse anti-Flag	Sigma-Aldrich	Cat#: F3165; RRID: AB_259529
Goat anti-Rabbit-IgG HRP	Sigma-Aldrich	Cat#: A0545; RRID: AB_257896
Goat anti-Mouse-IgG HRP	Millipore	Cat#: AP124P; RRID: AB_90456
Goat anti-Rabbit IgG (H+L) Secondary Antibody, Alexa Fluor 546	Thermo Fisher Scientific	Cat#: A-11010; RRID: AB_2534077
Goat anti-Mouse IgG (H+L) Secondary Antibody, Alexa Fluor 488	Thermo Fisher Scientific	Cat#: A28175; RRID: AB_2536161
Goat anti-Mouse IgG (H+L) Secondary Antibody, Alexa Fluor 594	Thermo Fisher Scientific	Cat#: A-21125; RRID: AB_2535767
Goat anti-Mouse IgG (H+L) Secondary Antibody, Alexa Fluor 680	Thermo Fisher Scientific	Cat#: A-21057; RRID: AB_2535723
Goat anti-Rabbit IgG (H+L) Secondary Antibody, Alexa Fluor 680	Thermo Fisher Scientific	Cat#: A-21109; RRID: AB_2535758
Chemicals, Peptides, and Recombinant Proteins		
Trizol	Invitrogen	Cat#: 15596018
SuperScript II	Invitrogen	Cat#: 18064014
Lipofectamin 3000	Thermo Fisher Scientific	Cat#: L30015
Lipofectamin 2000	Thermo Fisher Scientific	Cat#: 11668019
T-Pro NTR II transfection reagents	T-Pro Biotechnology	Cat#: JT97-N002M
Immobilon western chemiluminescent HRP substrate	Millipore	Cat#: WBKLS0500
Protease Inhibitor Cocktail Taclets	Thermo Fisher Scientific	Cat#: 4693159001
Phosphatase Inhibitor Cocktail Taclets	Thermo Fisher Scientific	Cat#: 4906837001
DAPI (4',6-Diamidino-2-Phenylindole, Dihydrochloride)	Thermo Fisher Scientific	Cat#: D1306
Critical Commercial Assays		
TruSeq RNA Library Prep Kit v2	Illumina	Cat#: RS-122-2001
RNA Clean and Concentrator	Zymo Research	Cat#: R1014
NimbleGen SeqCap EZ Exome v3.0	Roche	Cat#: 06465692001
QuikChange II Site-Directed Mutagenesis Kit	Agilent	Cat#: 200524
Pierce BCA Protein Assay Kit	Thermo Fisher Scientific	Cat#: 23225

REAGENT or RESOURCE	SOURCE	IDENTIFIER
Experimental Models: Cell Lines		
IM-9 lymphoblastoid cell line	Food Industry Research and Development Institute, Taiwan	Cat#: 60115
Patient derived lymphoblastoid cell lines	Food Industry Research and Development Institute, Taiwan	N/A
HEK293T	ATCC	Cat#: CRL-3216
U2OS	ATCC	Cat#: HTB-96
Oligonucleotides		
See Table S2	N/A	N/A
Recombinant DNA		
Flag-CEP85L	GeneScript	Cat#: OHu14925D
Flag-cep85l	GeneScript	Cat#: OMu02650C
HA-CEP85L	This Paper	N/A
Software and Algorithms		
STAR v.2.2.1	Dobin et al., 2013	https://github.com/alexdobin/STAR
GATK v3.1.1	DePristo et al., 2011	https://gatk.broadinstitute.org
BWAv0.7.8	Li and Durbin, 2009	http://bio-bwa.sourceforge.net/
gnomAD v2.1.1	N/A	https://gnomad.broadinstitute.org/
SeattleSeq v138	Ng et al., 2009	https://snp.gs.washington.edu/SeattleSeqAnnotation138/
Galaxy	NA	https://usegalaxy.org
wANNOVAR	NA	http://wannovar.wglab.org
Homo sapience genome GRCh37/hg19	N/A	N/A
ImageJ	NIH	https://imagej.nih.gov/ij/
ZEN Microscope Software	Zeiss	N/A
Other		
LSM-700 confocal	Zeiss	N/A
VT1000 S Vibrating blade microtome	Leica	N/A
Upright microscope (Axio imager. M2 440 ApoTome2 sysyem)	Zeiss	N/A
Fujifilm LAS-4000	Fujifilm	N/A